

## Accepted Manuscript

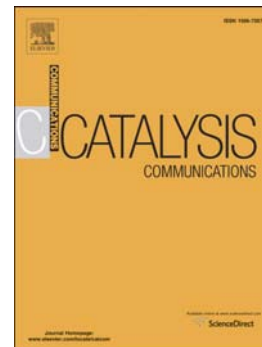
Cyclohexane dehydrogenation over Ni-Cu/SiO<sub>2</sub> catalyst: Effect of copper addition

Zhijun Xia, Hanfeng Lu, Huayan Liu, Zekai Zhang, Yinfei Chen

PII: S1566-7367(16)30404-6  
DOI: doi: [10.1016/j.catcom.2016.10.036](https://doi.org/10.1016/j.catcom.2016.10.036)  
Reference: CATCOM 4845

To appear in: *Catalysis Communications*

Received date: 19 July 2016  
Revised date: 1 October 2016  
Accepted date: 25 October 2016



Please cite this article as: Zhijun Xia, Hanfeng Lu, Huayan Liu, Zekai Zhang, Yinfei Chen, Cyclohexane dehydrogenation over Ni-Cu/SiO<sub>2</sub> catalyst: Effect of copper addition, *Catalysis Communications* (2016), doi: [10.1016/j.catcom.2016.10.036](https://doi.org/10.1016/j.catcom.2016.10.036)

This is a PDF file of an unedited manuscript that has been accepted for publication. As a service to our customers we are providing this early version of the manuscript. The manuscript will undergo copyediting, typesetting, and review of the resulting proof before it is published in its final form. Please note that during the production process errors may be discovered which could affect the content, and all legal disclaimers that apply to the journal pertain.

## Cyclohexane dehydrogenation over Ni-Cu/SiO<sub>2</sub> catalyst: Effect of copper addition

Zhijun Xia, Hanfeng Lu, Huayan Liu, Zekai Zhang, Yinfei Chen\*

Institute of Catalytic Reaction Engineering, College of Chemical Engineering, Zhejiang University of Technology, Hangzhou 310014, PR China

Zhijun Xia

E-mail address: xiazj919@163.com

Hanfeng Lu

E-mail address: luhf@zjut.edu.cn

Huayan Liu

E-mail address: hylu@zjut.edu.cn

Zekai Zhang

E-mail address: zzk@zjut.edu.cn

Yinfei Chen\*

\*Corresponding author. Tel: +86-13606643528, E-mail address: chfy@zjut.edu.cn

**Abstract:** A series of Ni-Cu/SiO<sub>2</sub> catalysts were prepared by sol-gel method for use in the dehydrogenation of cyclohexane to evolve hydrogen. The Ni/SiO<sub>2</sub> catalyst exhibits excellent catalytic activity but low selectivity, due to the highly dispersion of Ni species. After the addition of Cu, the Ni-Cu nanoparticles with narrow size distribution (3-6 nm) and a uniform structure of bimetallic Ni and Cu has been formed, and it drastically improves the selectivity to benzene. A 94.9% conversion of cyclohexane with 99.5% benzene selectivity was observed at 350 °C in a continuous fixed bed flow reactor.

**Keywords:** Cyclohexane dehydrogenation; Bimetallic catalysts; Nickel; Copper.

## 1. Introduction

Liquid organic hydrides, such as cyclohexane, methylcyclohexane and decalin and so on, have been potential industrial candidates for safe and efficient hydrogen storage and transport medium, due to its advantages of high hydrogen storage density, easy transportation, recyclable, CO-free and no greenhouse-gas CO<sub>2</sub> emission [1-3]. As the reverse reaction of hydrogenation, supported precious metal Pt catalysts which have good hydrogenation activity can also catalyze dehydrogenation of cycloalkanes, because of their ability to selectively functionalize C-H bond cleavage and poor ability to break undesired C-C bond [4-8]. To reduce Pt metal content or to improve the performance of dehydrogenation activity, addition of non-precious metal such as Mo [8], Ni [9] and Sn [10-12] to Pt based catalysts has been attempted. Furthermore, no-noble metal Ni and its bi-metallic catalysts for dehydrogenation reaction of cycloalkanes have attracted much attention [13-19].

However, Ni based or Ni alloy based catalysts exhibit a high hydrogenolysis activity [19-21], and a low selectivity for dehydrogenation of cycloalkanes. Great efforts have been made in improving the performance of Ni-based catalysts by adding a second metal. Al-ShaikhAli et al. [15] reported above 93.2% of toluene selectivity with methylcyclohexane conversions only 9.8~32.2% over the nickel-based bimetallic catalysts with Sn, Zn and In. A lower selectivity of 75% was exhibited over the Ni-Cu/C catalysts reported by Patil and co-workers [16]. Nevertheless, the effect of little active sites of Ni formed due to the poor interfaces of Ni and Cu can't be eliminated completely, except to totally change local structure of the Ni-based catalyst with a appropriate technology.

It is well known that, the crystal structures of copper and nickel are face-centered cubic (fcc), and have closed atomic size [22]. The addition of Cu to Ni-based catalysts in significant changes in selectivity in other reaction systems, due to the uniform structure or alloys of Ni and Cu [23,24]. In addition, sol-gel synthesis has a significant advantages of highly dispersing metals on gels of finely texture [25-27]. In this work, this method has been adopted to disperse Ni and Cu on SiO<sub>2</sub> to be a good contact for them and avoid the formation of the monometallic Ni, and the influence of Cu addition on the physicochemical properties and catalytic activities of Ni/SiO<sub>2</sub> catalysts in dehydrogenation of cyclohexane was investigated. The results indicate an unprecedented high selectivity in comparison with the monometallic Ni/SiO<sub>2</sub> catalysts.

## 2. Experimental

### 2.1 Catalyst preparation

The catalysts used in this study were prepared by the sol-gel method. Typically, to 40 mmol tetraethylorthosilicate (TEOS, Shanghai Wulian Chemical Factory) dissolved with 100 mL of deionized water (DI water), 0.1 g of citric acid monohydrate (Sinopharm Chemical Reagent Co.) was added with vigorously stirring at 40 °C water bath for 30 min to get a homogeneous solution. The total 10 mmol of nitrate (Ni(NO<sub>3</sub>)<sub>2</sub>·6H<sub>2</sub>O and Cu(NO<sub>3</sub>)<sub>2</sub>·3H<sub>2</sub>O, Sinopharm Chemical Reagent Co.) was added under stirring. After 1 h, an appropriate amount of a 10% by volume NH<sub>4</sub>OH aqueous solution was dropwise added to the mixed solution to form gel. The resulting gelatinous material was mixed immediately with 50 ml of DI water, and then kept 40 °C for 2 h. The product was filtered, washed with DI water 3 times, dried at 110 °C for 12 h, and calcined in air at 550 °C for 4 h.

### 2.2 Catalyst characterization

The specific surface area and porosity of all the samples were calculated from the nitrogen adsorption-desorption isotherms at -196 °C with a Micromeritics 3Flex Surface Characterization Analyzer. And the X-ray diffraction (XRD) patterns were collected in the 2θ range of 10°-80° on a PANalytical X'pert PRO diffractometer with Cu Kα (λ = 0.154 nm). The actual contents of Ni and Cu elements were determined by X-ray Fluorescence (XRF) spectroscopy with a EDX 3200S PLUS C spectrometer (Skyray Instrument). Diffuse reflectance UV-Visible (DR UV-Vis) spectra of the catalysts were recorded on a UV-2600 (Shimadzu) spectrophotometer, and collected in the

wave length of 200-800 nm at room temperature. A high-resolution transmission electron microscopy (HRTEM) study was performed with a Philips-FEI Tecnai G2 F30 S-Twin instrument operated at 300kv.

### 2.3 Catalytic reaction

The dehydrogenation of cyclohexane was carried out in a fixed bed flow reactor in a temperature range of 275-375 °C at atmospheric pressure. Typically, 150 mg of the catalyst precursor (40-60 mesh) was placed in between two quartz wool plugged in the center of the 5 mm (Internal Diameter) quartz reactor. Before the reaction, the catalyst was reduced in a flow of 30 mL min<sup>-1</sup> H<sub>2</sub> at 350 °C and atmospheric pressure for 4 h. The gas hourly space velocity (GHSV) was 12000 mL g<sup>-1</sup> h<sup>-1</sup> with a molar ratio of C<sub>6</sub>H<sub>12</sub> : H<sub>2</sub> = 1 : 25. Cyclohexane was introduced to the reactor system by bubbling H<sub>2</sub>, through buffer bottle at 0 °C ice water bath. The outlet stream was sampled using an automatic Valco 6 port valve system, and then analyzed over an online gas chromatography (Agilent GC-7890A, equipped with FID and a capillary column, HP-INNOWax).

The conversion of cyclohexane and the selectivity to benzene were calculated as:

$$\text{Conversion(\%)} = \frac{(\text{Moles of cyclohexane reacted})}{(\text{Moles of cyclohexane in feed})} \times 100\%.$$
$$\text{Selectivity(\%)} = \frac{(\text{Moles of product defined})}{(\text{Moles of cyclohexane reacted})} \times 100\%.$$

## 3. Results and discussion

### 3.1 Catalyst characterization

The textural properties of all catalysts prepared are presented in Table 1. The BET surface areas decrease while the content of Cu increase. Compared with Cu/SiO<sub>2</sub> catalyst, the pore volumes and average pore diameters of other catalysts are not apparent different. The Cu/SiO<sub>2</sub> catalyst have the minimum BET surface of 278.5 m<sup>2</sup> g<sup>-1</sup>, and the maximum pore volumes and average pore diameters. However, the content of Ni and Cu are also close to the expected value.

The XRD patterns of the spent catalysts after reduction in H<sub>2</sub> flow are shown in Fig. 1. Only an extremely weak signal observed confirm a high dispersion of Ni or Cu at about a 20% molar content of overall metals in the catalysts. And the XRD patterns of the fresh catalysts (see Fig. S1 of the Spplimentary Material) have not any peaks at all. This is caused by the strong metal-support interaction in the form of phyllosilicate between the metal (Ni or Cu) and SiO<sub>2</sub> [29], and the small and highly dispersion colloidal suspension of solid particles formed during the silica

sol-gel process [30].

The morphologies and structural details of the bimetallic Ni-Cu nanoparticles in the  $\text{Ni}_{0.85}\text{Cu}_{0.15}/\text{SiO}_2$  catalyst were examined by TEM (Fig. 2). The metallic or metallic oxide particles in the catalyst are well distributed uniformly, and no aggregation to form larger particles during the reduction process at 350 °C. Due to the similarities of the lattice parameters of Ni and Cu, it is difficult to distinguish between them, although a little clear lattice fringes have been observed in the high resolution (5nm) TEM images (Fig. 2c or Fig. 2d). The similarities between elemental maps of Cu-K and Ni-K exists in the HAADF images (Fig. 2e, more images can be found in Supplementary Material Fig. S3). And the atoms of Ni and Cu are in coexistence at an optional place (Fig. S4). These indicate a good fusion performance of Ni and Cu in the  $\text{Ni}_{0.85}\text{Cu}_{0.15}/\text{SiO}_2$  catalyst, and the Ni-Cu samples are not a total intermetallic alloys which was also reported in the previous work [24]. Furthermore, the detail particle sizes distributions for the fresh and spent  $\text{Ni}_{0.85}\text{Cu}_{0.15}/\text{SiO}_2$  catalyst obtained from TEM images are within 3-6 nm and 2-5 nm respectively (Fig. S2). These conclusions are in good agreement with the XRD results.

Fig. 3 presents the UV-Visible diffuse reflectance spectra of the fresh and spent catalysts. The  $B_2$  absorption band of  $\text{SiO}_2$  is located at about 240 nm [31]. It was found at around 370 nm related to oxidized nickel nanoparticles, and a broad absorption band at 550-700 nm related to absorption of nanostructures containing  $\text{Ni}^{2+}$  ions [32, 33]. The fresh Ni-contained catalysts and the spent  $\text{Ni}/\text{SiO}_2$  catalyst show a main absorption peak 425 nm and a broad absorption band at 600-750 nm, and display a distinct redshift due to the strong interaction between the metal Ni and support. After reduction and reaction, the high fraction of edge and corner Ni atoms in the spent  $\text{Ni}/\text{SiO}_2$  catalyst were easily oxidized to oxides [34]. Both of the spent  $\text{Ni}/\text{SiO}_2$  or  $\text{Cu}/\text{SiO}_2$  show a broad absorption band at 600-750 nm. However, no noticeable peak or absorption band can be observed in the wavelength range of 450-800 nm (Fig. 3B) in the spectra of the spent bimetallic Ni-Cu catalysts. This result also indicates that the uniform structure of bimetallic catalysts was formed after the introduction of Cu.

### 3.2 Catalytic activity

Fig.4 shows the catalytic dehydrogenation performance of  $\text{Ni}_x\text{Cu}_{1-x}/\text{SiO}_2$  catalysts. Compare with the bimetallic Ni-Cu catalysts, the monometallic  $\text{Ni}/\text{SiO}_2$  catalyst exhibits a substantially high cyclohexane conversion and a poor benzene selectivity with amounts of hydrogenolysis

products methane at above 325 °C, in agreement with previously reported dehydrogenation reaction tests over Ni-based catalysts [17]. And the Cu/SiO<sub>2</sub> catalyst shows close to 100% benzene selectivity from 275 °C to 375 °C, while its conversion of cyclohexane increases from 6.8% to 61.2%. All of the bimetallic Ni-Cu catalysts supported SiO<sub>2</sub> show a good selectivity of above 97% to benzene, and a high conversion which is close to that of Ni/SiO<sub>2</sub> catalyst. The Ni<sub>0.85</sub>Cu<sub>0.15</sub>/SiO<sub>2</sub> catalyst presents the highest yield of benzene (Fig. S5) with 94.9% cyclohexane conversion and 99.5% benzene selectivity at 350 °C, and appears to be very similar to the precious metal Pt catalysts [10, 15]. These results clearly indicate that the introduction of copper beside nickel in the Ni/SiO<sub>2</sub> catalyst drastically improve the chemoselectivity to benzene for the dehydrogenation reaction of cyclohexane.

These variations in the activities depend on the physicochemical and structural properties of the catalysts. The formation of a considerable amount of active sites is significant for the dehydrogenation activity due to the high dispersion and small metal crystallites in the catalysts of this work. The small metal Ni particles are more active for C-H bond and C-C bond activation than Cu particles, due to their partially filled d-band [16] and highly dissociative chemisorption energies [35]. With higher temperature, this activity would be more easy to active the C-C bond. The addition of Cu to Ni decreased the activity, and led to an incredible increase of dehydrogenation selectivity to benzene according to the Sabatier principle. Furthermore, to avoid carbon deposit, the applications of the neutral support SiO<sub>2</sub> and the carrier gas H<sub>2</sub> are advantages for the stability of the catalyst.

#### 4. Conclusions

As described above, it is inferred that the sol-gel method was favorable for obtaining the high metal dispersion in the SiO<sub>2</sub> supported bimetallic Ni-Cu catalysts. These catalysts presents a outstanding performance for cyclohexane dehydrogenation, and a good selectivity especially due to the addition of copper. An appropriate design of the Ni-Cu interface is clearly a viable strategy for the development of more effective no-precious metal catalysts for cyclohexane dehydrogenation.

#### Appendix A. Supplementary data

Supplementary data associated with this article could be found, in the online version, at xxxx.

**References**

- [1] F. Alhumaidan, D. Cresswell, A. Garforth, *Energy Fuels* 25 (2011) 4217-4234.
- [2] D.J. Durbin, C. Malardier-Jugroot, *International Journal of Hydrogen Energy* 38 (2013) 14598-14617.
- [3] A.U. Pradhan, A. Shukla, J.V. Pande, S. Karmarkar, R.B. Biniwale, *International Journal of Hydrogen Energy* 36 (2011) 680-688.
- [4] P. Li, Y.L. Huang, D. Chen, J. Zhu, T.J. Zhao, X.G. Zhou, *Catalysis Communications* 10 (2009) 815-818.
- [5] G. Lee, Y. Jeong, B.G. Kim, J.S. Han, H. Jeong, H.B. Na, J.C. Jung, *Catalysis Communications* 67 (2015) 40-44.
- [6] N. Jiang, K.S.R. Rao, M.-J. Jin, S.-E. Park, *Applied Catalysis A: General* 425-426 (2012) 62-67.
- [7] B. Wang, G.F. Froment, D.W. Goodman, *Journal of Catalysis* 253 (2008) 239-243.
- [8] N. Boufaden, R. Akkari, B. Pawelec, J.L.G. Fierro, M.S. Zina, A. Ghorbel, *Journal of Molecular Catalysis A: Chemical* 420 (2016) 96-106.
- [9] S. Qi, Y. Li, J. Yue, H. Chen, C. Yi, B. Yang, *Chinese Journal of Catalysis* 35 (2014) 1833-1839.
- [10] E. Gianotti, M. Taillades-Jacquín, A. Reyes-Carmona, G. Taillades, J. Roziere, D.J. Jones, *Applied Catalysis B: Environmental* 185 (2016) 233-241.
- [11] E. Gianotti, A. Reyes-Carmona, M. Taillades-Jacquín, G. Taillades, J. Roziere, D.J. Jones, *Applied Catalysis B: Environmental* 160-161 (2014) 574-581.
- [12] C. Lucarelli, S. Albonetti, A. Vaccari, C. Resini, G. Taillades, J. Roziere, K.-E. Liew, A. Ohnesorge, C. Wolff, I. Gabellini, D. Wails, *Catalysis Today* 175 (2011) 504-508.
- [13] S. Qi, J. Yue, Y. Li, J. Huang, C. Yi, B. Yang, *Catalysis Letters* 144 (2014) 1443-1449.
- [14] N. Boufaden, R. Akkari, B. Pawelec, J.L.G. Fierro, M.S. Zina, A. Ghorbel, *Applied Catalysis A: General* 502 (2015) 329-339.
- [15] A.H. Al-ShaikhAli, A. Jedidi, L. Cavallo, K. Takanabe, *Chemical Communications* 51 (2015) 12931-12934.
- [16] S.P. Patil, J.V. Pande, R.B. Biniwale, *International Journal of Hydrogen Energy* 38 (2013) 15233-15241.



- [17] J. Escobar, J.A.D.L. Reyes, T. Viveros, M.C. Barrera, *Industrial & Engineering Chemistry Research* 45 (2006) 5693-5700.
- [18] M.V.P. Sharma, J.F. Akyurtlu, A. Akyurtlu, *International Journal of Hydrogen Energy* 40 (2015) 13368-13378.
- [19] L. Zhang, G. Xu, Y. An, C.P. Chen, Q. Wang, *International Journal of Hydrogen Energy* 31 (2006) 2250-2255.
- [20] P. H. Desai, J.T. Richardson, *Journal of Catalysis* 98 (1986) 392-400.
- [21] J.H. Sinfelt, J.L. Carter, D.J.C. Yates, *Journal of Catalysis* 24 (1972) 283-296.
- [22] E.C.M. Chen, J.G. Dojahn, W.E. Wentworth, *The Journal of Physical Chemistry A* 101 (1997) 3088-3101.
- [23] S. A. Khromova, A.A. Smirnov, O.A. Bulavchenko, A.A. Saraev, V.V. Kaichev, S.I. Reshetnikov, V.A. Yakovlev, *Applied Catalysis A: General* 470 (2014) 261-270.
- [24] B.C. Miranda, R.J. Chimentao, J. Szanyi, A.H. Braga, J.B.O. Santos, F. Gispert-Guirado, J. Llorca, F. Medina, *Applied Catalysis B: Environmental* 166-167 (2015) 166-180.
- [25] G. Goncalves, M.K. Lenzi, O.A.A. Santos, L.M.M. Jorge, *Journal of Non-Crystalline Solids* 352 (2006) 3697-3704.
- [26] J. Escobar, J.A.D.L. Reyes, T. Viveros, *Applied Catalysis A: General* 253 (2003) 151-163.
- [27] C. Louis, Z.X. Cheng, M. Che, *The Journal of Physical Chemistry* 1993, 197(21): 5703-5712.
- [28] J.-H. Kim, D.J. Sub, T.-J. Park, K.L. Kim. *Applied Catalysis A: General*, 197(2000), 191-200.
- [29] W. Di, J. Cheng, S. Tian, J. Li, J. Chen, Q. Sun. *Applied Catalysis A: General* 510 (2016) 244-259.
- [30] J. Regalbuto, *Catalyst Preparation Science and Engineering*, CRC Press, Boca Raton, 2007.
- [31] C.D. Marshall, J.A. Speth, S.A. Payne, *Journal of Non-Crystalline Solids* 212 (1997) 59-73.
- [32] X. Xiang, X.T. Zu, S. Zhu, C.F. Zhang, L.M. Wang, *Nuclear Instruments and Methods in Physics Research B* 250 (2006) 229-232.
- [33] G. Carja, A. Nakajima, C. Dranka, K. Okada, *Journal of Nanoparticle Research* 12 (2010) 3049-3056.
- [34] J. Zhou, X. Duan, L. Ye, J. Zheng, M.M.-J. Li, S.C.E. Tsang, Y. Yuan, *Applied Catalysis A:General* 505 (2015) 344-353.
- [35] T. Bligaard, J.K. Norskov, S. Dahl, J. Matthiesen, C.H. Christensen, J. Sehested, *Journal of*

Catalysis 224 (2004), 206-217.

ACCEPTED MANUSCRIPT

## List of Tables

Table 1 The physicochemical properties of  $\text{Ni}_x\text{Cu}_{1-x}/\text{SiO}_2$  catalysts

## List of Figures

**Fig. 1.** XRD patterns of the spent  $\text{Ni}_x\text{Cu}_{1-x}/\text{SiO}_2$  catalysts. (a)  $\text{Ni}/\text{SiO}_2$ , (b)  $\text{Ni}_{0.90}\text{Cu}_{0.10}/\text{SiO}_2$ , (c)  $\text{Ni}_{0.85}\text{Cu}_{0.15}/\text{SiO}_2$ , (d)  $\text{Ni}_{0.80}\text{Cu}_{0.20}/\text{SiO}_2$ , (e)  $\text{Cu}/\text{SiO}_2$ .

**Fig. 2.** TEM images of  $\text{Ni}_{0.85}\text{Cu}_{0.15}/\text{SiO}_2$  catalysts. (a and c) fresh and (b and d) spent catalyst, (e) HAADF-STEM images of the spent catalyst, Cu-K (yellowgreen) and Ni-K (red).

**Fig. 3.** UV-Vis DRS spectra of  $\text{Ni}_x\text{Cu}_{1-x}/\text{SiO}_2$  catalysts. (A) fresh and (B) spent catalysts. (a)  $\text{Ni}/\text{SiO}_2$ , (b)  $\text{Ni}_{0.90}\text{Cu}_{0.10}/\text{SiO}_2$ , (c)  $\text{Ni}_{0.85}\text{Cu}_{0.15}/\text{SiO}_2$ , (d)  $\text{Ni}_{0.80}\text{Cu}_{0.20}/\text{SiO}_2$ , (e)  $\text{Cu}/\text{SiO}_2$ .

**Fig. 4.** Catalytic performance of  $\text{Ni}_x\text{Cu}_{1-x}/\text{SiO}_2$  catalysts.

Table 1

The physicochemical properties of Ni<sub>x</sub>Cu<sub>1-x</sub>/SiO<sub>2</sub> catalysts

Catalysts	S <sub>BET</sub> (m <sup>2</sup> g <sup>-1</sup> )	Pore volume (cm <sup>3</sup> g <sup>-1</sup> )	Pore size (nm)	Metal loading <sup>a</sup> (mole%)	
				Ni	Cu
Ni/SiO <sub>2</sub>	462.9	0.40	3.45	20.89	0
Ni <sub>0.90</sub> Cu <sub>0.10</sub> /SiO <sub>2</sub>	401.8	0.35	3.50	18.39	2.42
Ni <sub>0.85</sub> Cu <sub>0.15</sub> /SiO <sub>2</sub>	396.0	0.38	3.81	17.32	3.59
Ni <sub>0.80</sub> Cu <sub>0.20</sub> /SiO <sub>2</sub>	354.6	0.34	3.82	16.81	4.46
Cu/SiO <sub>2</sub>	278.5	0.64	9.14	0	19.84

<sup>a</sup> Metal loading determined by XRF, a molar ratio of Ni or Cu/(metal + Si).

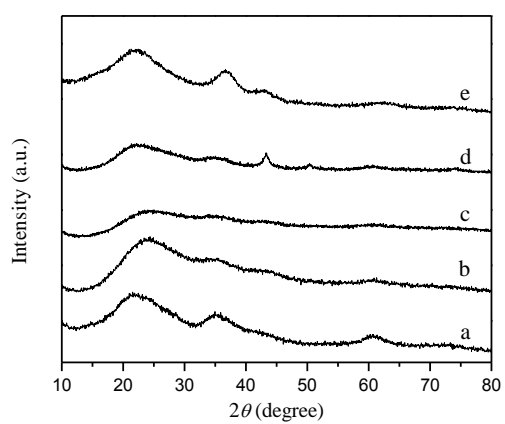


Fig. 1

ACCEPTED MANUSCRIPT

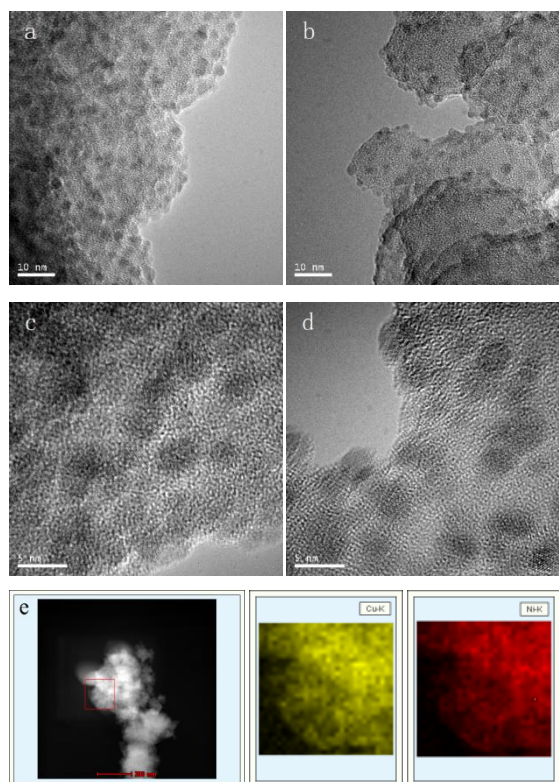


Fig. 2

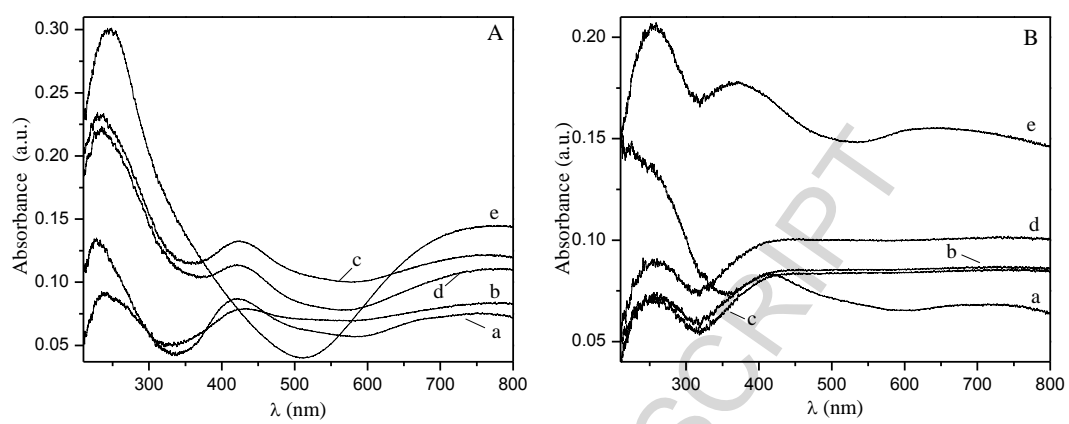


Fig. 3

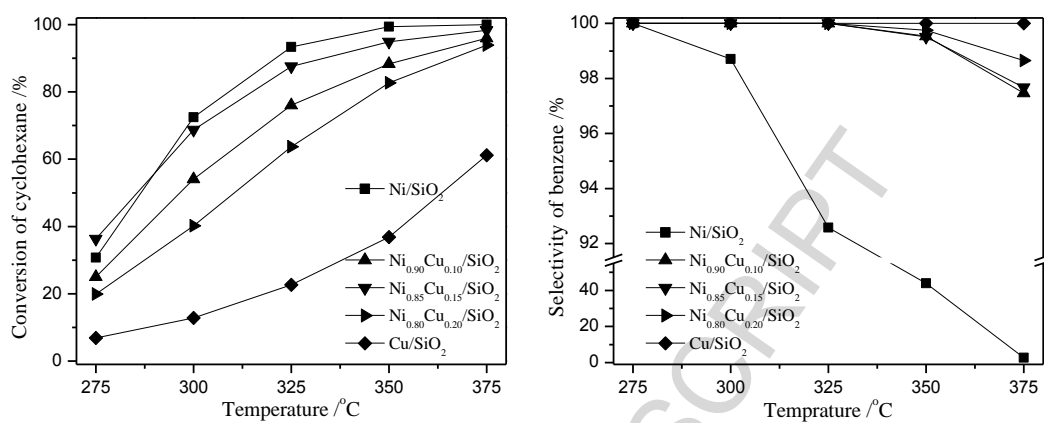
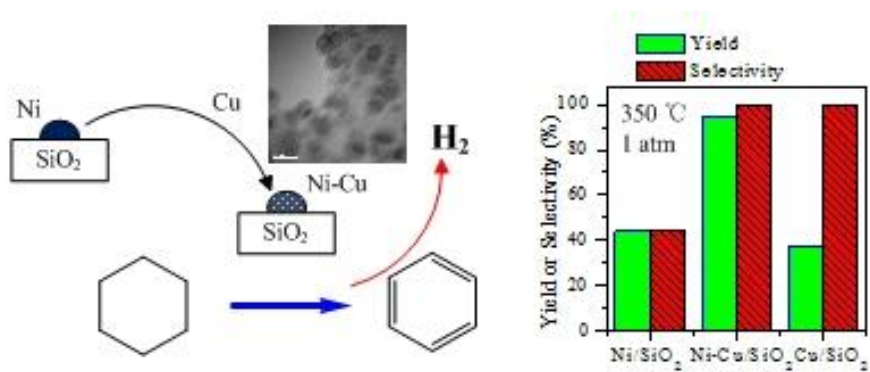


Fig. 4





Graphical abstract

**Highlights**

- > Highly dispersed metallic nanoparticles on SiO<sub>2</sub> were synthesized by sol-gel method.
- > Small Ni-Cu bimetallic nanoparticles uniform in composition.
- > A dramatic improvement of selectivity has been achieved by introduction of Cu beside Ni.
- > Ni-Cu/SiO<sub>2</sub> catalysts presented excellent activity for cyclohexane dehydrogenation.

ACCEPTED MANUSCRIPT